

Synthesis of 1D and 2 D Multi-beam Annular Microstrip Antenna Arrays by Adaptive Particle Swarm Optimization for TM_{11} and TM_{12}

HICHEM CHAKER¹, MEHADJI ABRI² AND HADJIRA ABRI BADAOU³

¹Department of Electronic, Sidi Bel Abbès University, Algeria

²Department of Telecom, Tlemcen University, Algeria

³STIC laboratory, Department of Telecom, Tlemcen University, Algeria

Department of Electronic, University of Sidi Bel Abbès, ALGERIA

ALGERIA

mh_chaker2005@yahoo.fr

Abstract: - This paper describes the original results obtained in the field of multi-beam annular ring antenna array pattern synthesis for the modes TM_{11} and TM_{12} , by applying an iterative algorithm for phased arrays, which is able to produce low side-lobe level patterns with multiple prescribed main lobes. The proposed method is based on the adaptive particle swarm optimization algorithm. This solution is characterized by its simple implementation and a reduced computational time to achieve the desired radiation patterns. These advantages make the presented algorithm suitable for a wide range of communication systems. The original results obtained in the field of antenna array pattern synthesis are presented and, several illustrative examples are simulated to verify the validity of the proposed method.

Key-Words: - Adaptive Particle Swarm Optimizer, Synthesis, Annular Ring Microstrip antenna, Multibeam Linear and Planar Antenna Arrays.

1 Introduction

Antenna arrays are becoming a very important component of modern communication systems because of the exhaustive technological improvement in this field and the rapidly rising requirements [1]. The annular ring has received considerable attention, when operated in its fundamental TM_{11} mode. This printed antenna is smaller than its rectangular or circular counterparts. The annular ring may also be somewhat broadband in nature when operated near the TM_{12} resonance [2]. It has been shown that the structure is a good resonator (with very little radiation) for TM_{1m} modes (m odd), and a good radiator for TM_{1m} modes (m even) [3]. As discussed in previous works, the recent meta-heuristic methods have found application in several communication systems, and have therefore increased the interest of the research community in the synthesis of microstrip antenna arrays [4-5]. The algorithms used must be able to produce radiation patterns with multiple main lobes to the desired directions and for some practical applications, should be able to perform the synthesis by acting on both parameters, i.e. the amplitudes and phases of excitations for the two modes TM_{11} and TM_{12} .

Among the large number of available amplitude-phase techniques, the solutions that produce patterns with multiple main lobes are usually developed for arrays having a square radiator [6-7].

In this paper, an efficient method for the pattern synthesis of linear and planar multibeam annular ring antenna arrays is presented. A multi beam pattern is achieved by finding the excitation magnitude and phase of each array element, for the two modes TM_{11} and TM_{12} . The proposed method is based on the adaptive particle swarm optimization, and the linear and planar antenna array synthesis was modeled as a mono-objective optimization problem. To verify the validity of the technique, several illustrative examples are simulated, and multi-beam patterns are demonstrated.

2 Theoretical Considerations

The far field annular ring antenna in the plane $(\vec{u}_\theta, \vec{u}_\varphi)$ is expressed by equations (1) and (2) [8].

$$E_{\theta} = -j^n \frac{E_0 e^{-jk_0 H_s}}{2r} \left\{ \begin{matrix} r_{2eq} A_n (K_0 r_{2eq} \sin \theta) F_{nm}(r_{2eq}) \\ -r_{1eq} A_n (K_0 r_{1eq} \sin \theta) F_{nm}(r_{1eq}) \end{matrix} \right\} \cos(n\varphi) \quad (1)$$

$$E_{\phi} = -j^n \frac{E_0 e^{-jk_0 H_s}}{2r} \left\{ \begin{matrix} r_{2eq} B_n (K_0 r_{2eq} \sin \theta) F_{nm}(r_{2eq}) \\ -r_{1eq} B_n (K_0 r_{1eq} \sin \theta) F_{nm}(r_{1eq}) \end{matrix} \right\} \sin(n\varphi) \cos \theta \quad (2)$$

The antenna characteristics are as follows: $\epsilon_r=2.32$; $H_s=1.59\text{mm}$; $r_1=35\text{mm}$; $r_2=70\text{mm}$.

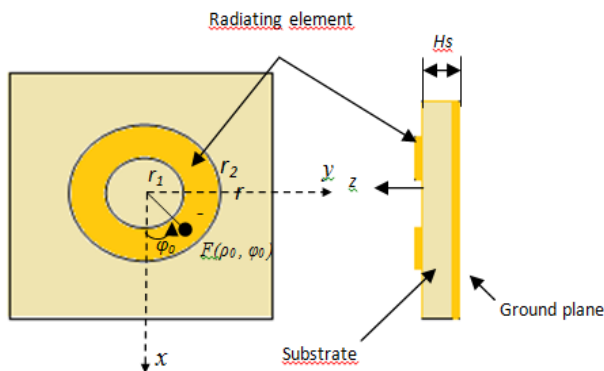


Fig.1 Geometry of a circular ring microstrip antenna

In this paper an annular-ring microstrip antenna is applied for TM_{11} and TM_{12} modes at the resonance frequencies 0.6 GHz and 2.6 GHz, respectively. An array antenna can be defined as a collection of individual elements in which the location and feeding are properly selected such that to enforce a desired far field pattern. Usually, array antennas are used when it is important to have a directive beam [9]. The far field radiated in free space from a linear array, composed of N identical sources of directivity diagram $\vec{f}(\theta, \varphi)$, each one localized at position x_i can be written as:

$$\vec{E}(M) = \sum_{i=1}^N \vec{E}_i(M) = \sum_{i=1}^N \vec{f}(\theta) \cdot \frac{w_i}{|S_i M|} e^{-j.k_0 |S_i M|} \quad (3)$$

Where k_0 is the wave number, θ and φ the angular directions, and $w_i = a_i e^{-j\varphi_i}$ the complex excitation.

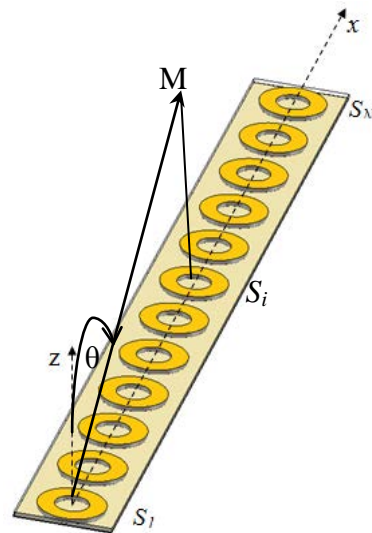


Fig.2 Linear ring antennas array

The directivity pattern $F(\theta, \varphi)$ is a function of the two direction angles θ and φ . If φ is fixed, the pattern $F(\theta, \varphi)$ could be conformed in the E plane or H plane. We are interested in the synthesis of linear arrays in the plane $\varphi = 0$. An antenna array, which consists of M rows and N columns of elements, arranged along a rectangular grid in the xoy plane, is shown in figure 3. The array has an element spacing of Δx in the x -direction and Δy in the y -direction. The far field can be expressed as follows:

$$F(\theta, \varphi) = f(\theta, \varphi) \sum_{m=1}^{N_x} \sum_{n=1}^{N_y} W_{mn} e^{j K_0 \sin \theta (X_m \cos \varphi + Y_n \sin \varphi)} \quad (4)$$

$$W_{mn} = W_m \times W_n \quad (5)$$

Where W_{mn} is the 2-D weight distribution of the array.

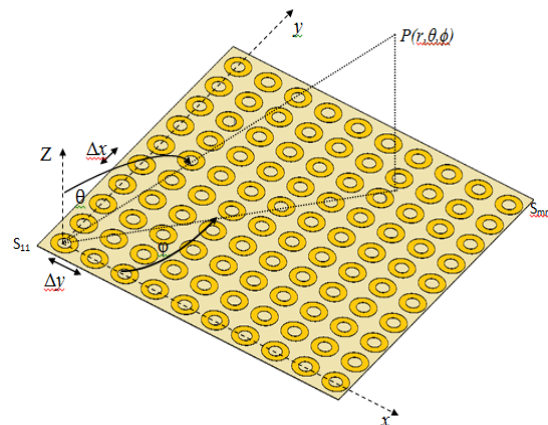


Fig.3 Element layout of uniform planar array.

The array factor in dB is given by:

$$P(\theta, \varphi) = 20 \text{Log}(F(\theta, \varphi)_{\text{normalised}}) \quad (6)$$

The mathematical statement of the optimization process is:

$$\text{Find } \max f(v) \rightarrow v_{\text{opt}} \quad (7)$$

Where $f(v)$ is the objective function of parameter variable v .

The optimization process can be modeled by minimizing the difference between the desired and calculated patterns. Mathematically, the optimization problem can be written as:

$$f = \text{Max} - \int_0^{\pi} |F_d(\theta, \varphi) - F(\theta, \varphi)| d\theta d\varphi \quad (8)$$

3 Adaptive Particle Swarm Algorithm

Modern heuristic algorithms are considered as practical tools for nonlinear optimization problems, which do not require the objective function to be differentiable or continuous. The particle swarm optimization (PSO) algorithm, as discussed by Xiao [10], is an evolutionary computation technique, which is inspired by social behavior of swarms. PSO is similar to the other evolutionary algorithms, i.e. the system is initialized with a population of random solutions. Each potential solution, or particle flies in a D-dimensional space with a dynamically adjusted speed. It is important to take into account the best position of the particle and the best positions of the particles of the neighborhood. The location of the i^{th} particle is represented as $X_i = (x_{i1}, \dots, x_{id}, \dots, x_{iD})$. The best previous position (which gives the best fitness value) of the i^{th} particle is recorded and represented as $P_i = (p_{i1}, \dots, p_{id}, \dots, p_{iD})$, which is also called *pbest*. The index of the best *pbest* among all the particles is represented by the symbol g . The location P_g is also called *gbest*. The velocity of the i^{th} particle is represented as $V_i = (v_{i1}, \dots, v_{id}, \dots, v_{iD})$. The particle swarm optimization consists of, at each time step, changing the velocity and location of each particle toward its *pbest* and *gbest* locations according to equations (9) and (10), respectively:

$$V_{id} = w \times V_{id} + C_1 \times \text{rand}() \times (p_{id} - x_{id}) + C_2 \times \text{rand}() \times (p_{gd} - x_{id}) \quad (9)$$

$$x_{id} = x_{id} + V_i \quad (10)$$

Where w is the inertia weight, c_1 and c_2 the acceleration constants, as discussed by Eberhart

[10], and $\text{rand}()$ is a random function in the range [0, 1]. In equation (9), the first part represents the inertia of the previous velocity; the second part is the cognition part, which represents the private thinking by itself, and the third part is the social part, which represents the cooperation among the particles, as discussed by Kennedy [11]. V_i is clamped to a maximum velocity $V_{\text{max}} = (v_{\text{max},1}, \dots, v_{\text{max},d}, \dots, v_{\text{max},D})$. V_{max} determines the resolution with which regions between the present and the target position are searched, as discussed by Eberhart [12]. The process for the implementation of PSO is as follows:

- Set the current iteration generation $G_c = 1$. Initialize a population which includes m particles. The i^{th} particle has a random position X_i in a specified space. For the d^{th} dimension of V_i , $v_{id} = \text{rand}_2() \times v_{\text{max},d}$, where $\text{rand}_2()$ is a random value in the range [-1, 1];
- Evaluate the fitness of each particle;
- Compare the evaluated fitness value of each particle with its *pbest*. If the current value is better than *pbest*, then set the current location as the *pbest* location. Furthermore, if the current value is better than *gbest*, then reset *gbest* to the current index in the particle array;
- Change the velocity and location of the particle according to the equations (9) and (10), respectively;
- $G_c = G_c + 1$, loop to step b) until a stop criterion is met. Usually a sufficiently good fitness value or G_c achieves a predefined maximum generation G_{max} .

The particle swarm optimization (PSO) includes the following parameters: number of particles m , inertia weight w , acceleration constants c_1 and c_2 , maximum velocity V_{max} . As evolution goes on, the swarm might undergo an undesired diversity loss. Some particles become inactive so they lose both the global and local search capabilities in the next generations. For a particle, the loss of global search capability means that it will be flying only within a quite small space, which will occur when its location and *pbest* are close to *gbest* (if the *gbest* has not significant changes) and when its velocity is close to zero for all dimensions. The loss of local search capability means that the possible flying cannot lead to a perceptible effect on its fitness. From the theory of self-organization, as discussed by Nicolis [13], if the system is going to be in equilibrium, the evolution process will stagnate. If *gbest* is located at a local optimum, then the swarm becomes premature convergence, as all the particles become inactive. To stimulate the swarm with sustainable development, the inactive particle should be adaptively replaced by a fresh one so as to

keep the non-linear relations of feedback in equation (9) efficient by maintaining the social diversity of the swarm. However, it is hard to identify the inactive particles, since the local search capability of a particle is highly depended on the specific location in the complex fitness landscape for different problems. Fortunately, the precision requirement for the fitness value is easily found from the fitness function. The adaptive PSO is executed by substituting step d) of the standard PSO process, by the pseudo code of the adaptive PSO that is shown in figure 4.

```

int[ ]similar Count = new int[m]; // at initialization stage
// Next code is employed to replace step d)
// in standard PSO process
For (i = 0; i < m; i++) { // for each particle
    IF (i ≠ g && |ΔFi| < ε)
        THEN similar Count[i]++; // add1
    ELSE similar Count[i] = 0; // reset
    IF (similar Count[i] > Tc) // predefined count
        THEN replace (the ith particle);
    ELSE execute (step d) in standard PSO
}
    
```

Fig.4 Inserted pseudo code of adaptive PSO

F_i is the fitness of the i^{th} particle, F_{gbest} is the fitness of $gbest$, $\Delta F_i = f(F_i, F_{gbest})$, $f(x)$ is an error function, ϵ a predefined critical constant, depending on the precision requirement. T_c is the count constant. The replace () function is used to replace the i^{th} particle, where X_i and V_i are reinitialized using the process in step a) of standard PSO, and its $pbest$ is equal to X_i . The array $similar\ Count[i]$ is employed to store the counts which successively satisfy the condition $|\Delta F_i| < \epsilon$ for the i^{th} particle which is not $gbest$. The inactive particle naturally satisfies the replace condition; however, if the particle is not inactive, it has less chance to be replaced as T_c increases.

For APSO, ΔF_i is set as a relative error function, which is $(F_i - F_{gbest}) / \text{Min}(\text{abs}(F_i), \text{abs}(F_{gbest}))$, where $\text{abs}(x)$ is the absolute value of x , $\text{Min}(x_1, x_2)$ the minimum value between x_1 and x_2 . The critical constant ϵ is set to 0.0001, and the count constant T_c to 3. For the problem at hand, the number of dimensions is equal to twice the number of antenna elements, because both the phase and position of each parameter must be specified by the PSO. A swarm of 40 particles was used. The algorithm parameters c_1 and c_2 specify the relative weight that the global best position has versus the particle's own best. Empirical testing has found that 0.5 is a reasonable value for both c_1 and c_2 . Linear velocity

damping was applied with the upper limit equal to 0.9. Velocity damping improves the convergence behavior of the particle swarm by gradually increasing the relative emphasis of the global and own best positions on a particle's velocity. The upper limit of the inertia weight is 0.9 and the lower limit is 0.4.

4 Numerical Results

The aim of the synthesis technique presented in this section is to optimize a multibeam linear uniform array in such a way that its main lobes occur exactly at some given angles, with maximum tolerance on the sidelobe level using complex weight excitations. The method has been applied to the design of eight uniform arrays for two modes TM_{11} and TM_{12} . The optimized design of multibeam antenna arrays is reported with numerical results.

The case of an array with 12 elements and $\lambda/2$ spacing is introduced. This array is supposed to generate two beams directed at the two angles 70° and 110° , for the two modes TM_{11} and TM_{12} , respectively. Figures 5 and 6 show the normalized output pattern in dB, and the relative amplitudes of the two beams are equal to unity for both modes. The maximum side-lobe levels are equal to -17.09 dB and -18.06 dB for the two modes TM_{11} and TM_{12} , respectively.

For the design specifications of amplitude-phase synthesis, the adaptive particle swarm optimizer (APSO) is run for 120 iterations and 200 iterations for the modes TM_{11} and TM_{12} , respectively, as shown in figures 7 and 8.

The distribution of the amplitude and phase excitation law of the radiating elements in the periodic array is shown in figure 9.

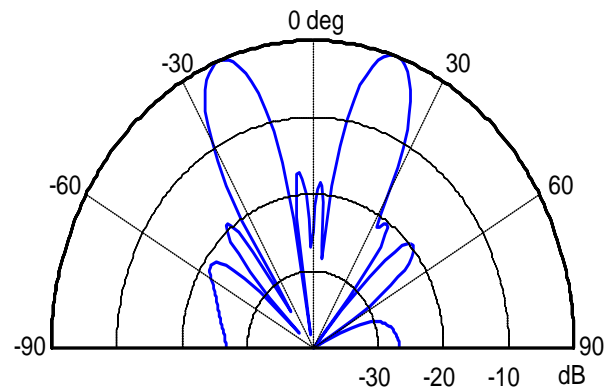


Fig.5 Normalized pattern TM_{11}

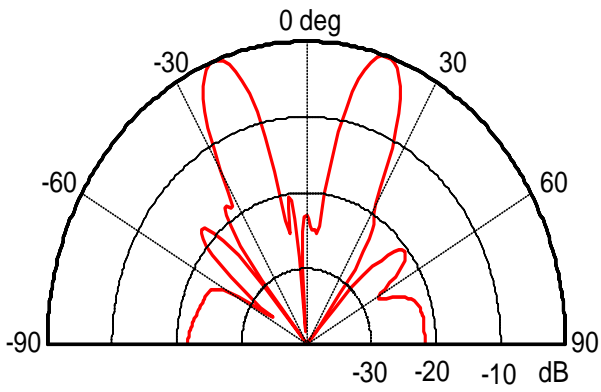


Fig.6 Normalized pattern TM_{12}

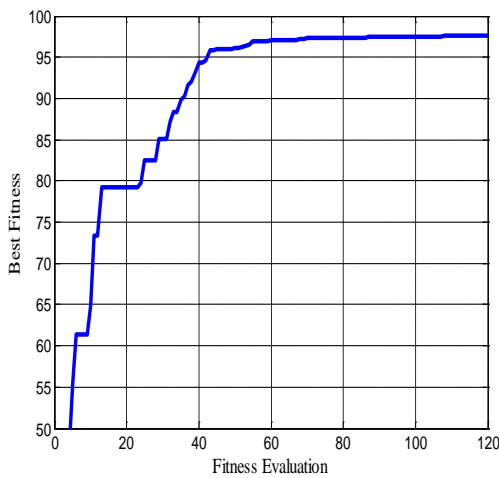


Fig.7 The convergence curve TM_{11} .

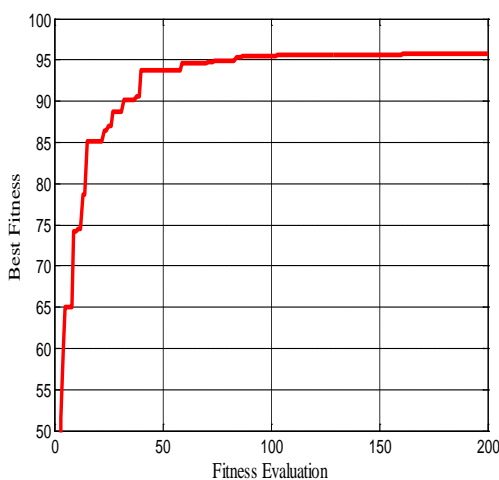


Fig.8 The convergence curve TM_{12} .

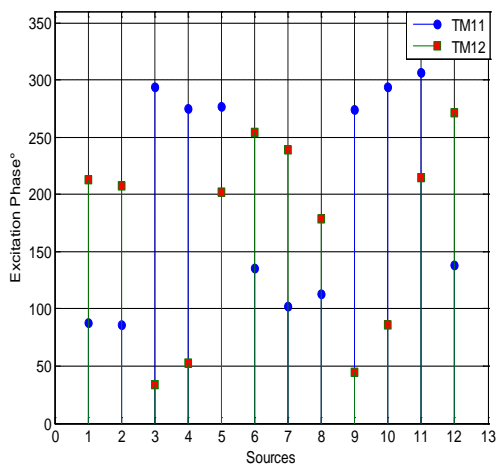
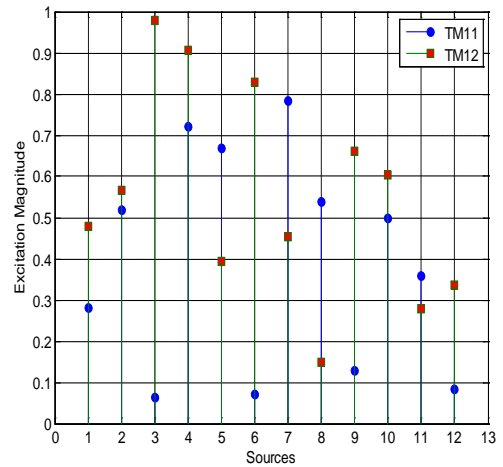


Fig.9 Excitation amplitudes and phases by APSO for the two modes.

The second example belongs to the synthesis of a 12 radiators linear array, where the amplitudes and phases are modified. The adaptive particle swarm optimization is able to produce patterns with two prescribed main lobes, at 90° and 110° for both modes TM_{11} and TM_{12} , while limiting the side-lobe level. The amplitude phase synthesis gave the maximum side lobe levels of -18 and -19.50 dB, for the two modes TM_{11} and TM_{12} , respectively. The adaptive particle swarm optimization was run for 100 iterations for the two modes with an initial population of 40 particles. The optimized excitation magnitudes and phases of the array elements are shown in figure 14.

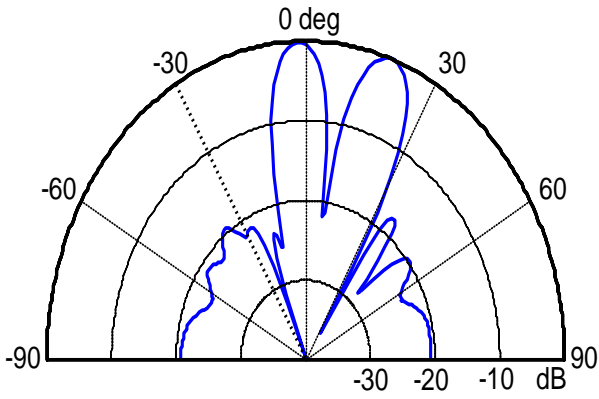


Fig.10 Normalized pattern TM₁₁

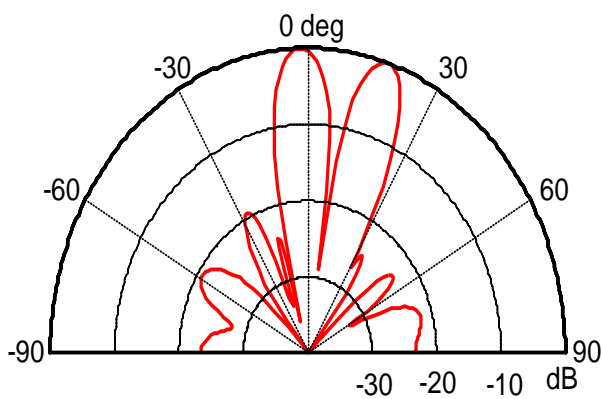


Fig.11 Normalized pattern TM₁₂.

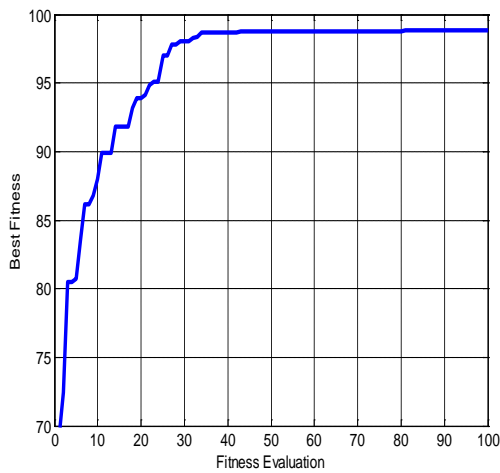


Fig.12 The convergence curve TM₁₁.

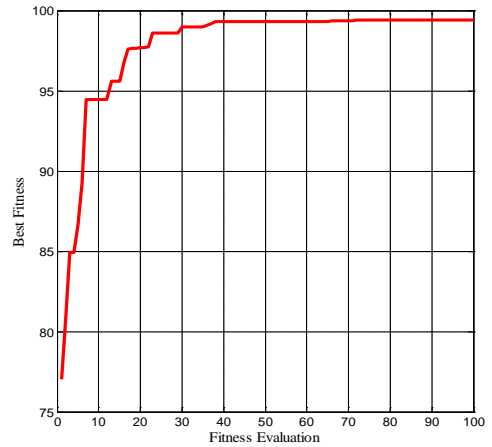


Fig.13 The convergence curve TM₁₂.

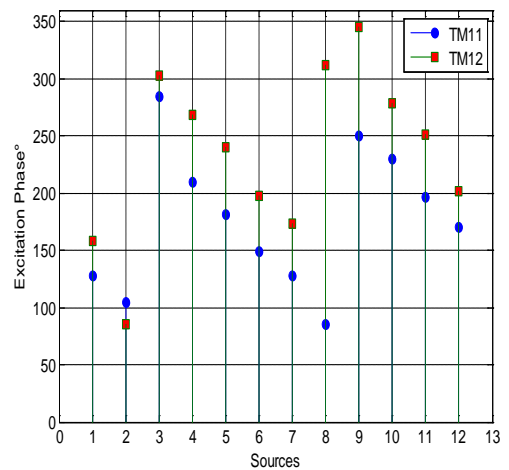
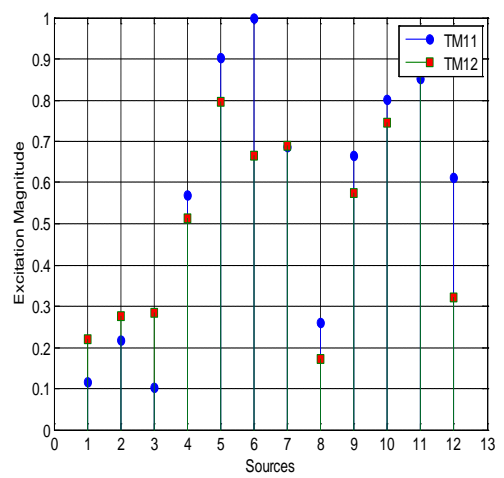


Fig.14 Excitation amplitudes and phases by APSO for the two modes.

The third numerical example refers to the same array and is obtained by imposing three maxima along the desired directions. It can be noticed that, when the proposed algorithm is used, the beams can be oriented exactly in the required directions. The

proposed method yielded the patterns shown in figures 15 and 16, for TM_{11} and TM_{12} modes, respectively. After 100 and 250 iterations, the fitness value reached its maximum and the optimization process ended due to meeting the design goal for both modes TM_{11} and TM_{12} . The fitness convergence curves are presented in figures 17 and 18. The synthesis results obtained for the two modes TM_{11} and TM_{12} are depicted in figure 19.

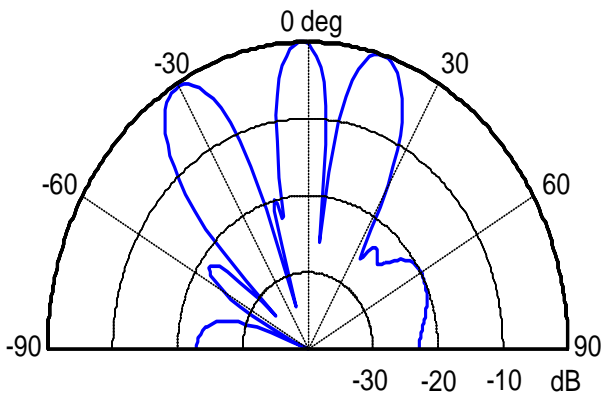


Fig.15 Normalized pattern TM_{11}

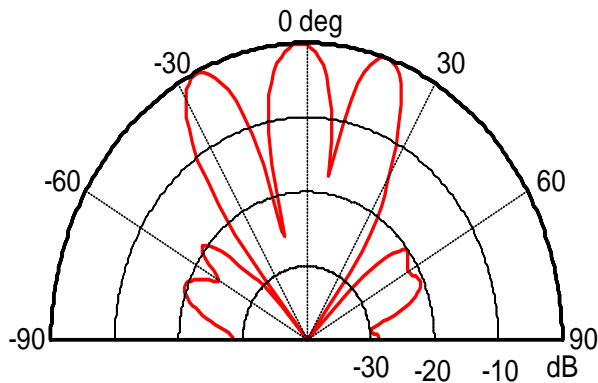


Fig.16 Normalized pattern TM_{12}

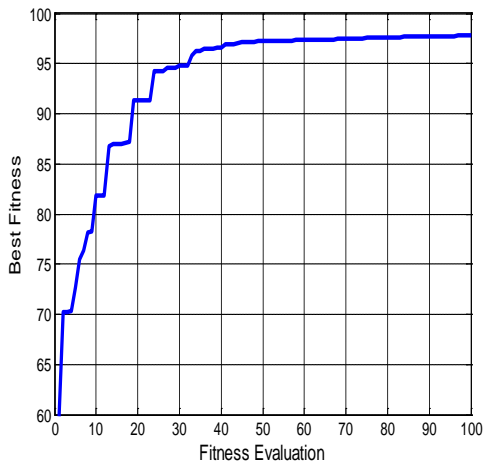


Fig.17 The convergence curve TM_{11}

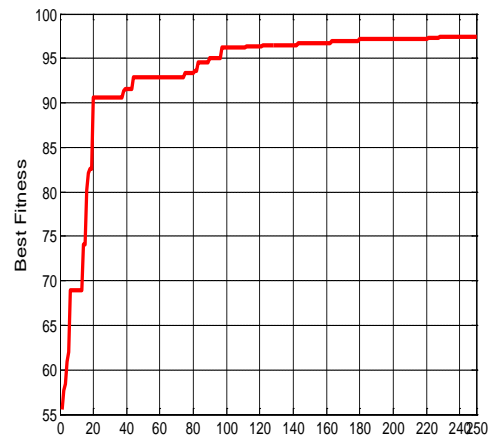


Fig.18 The convergence curve TM_{12} .

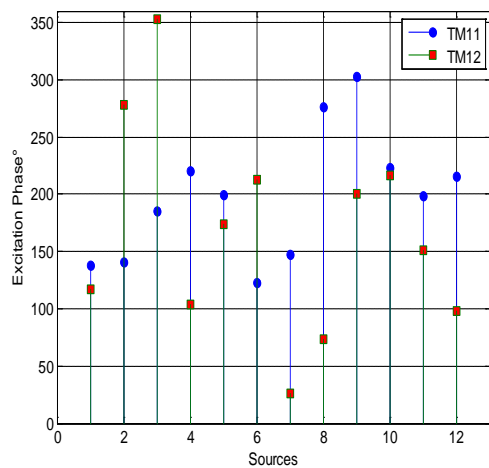
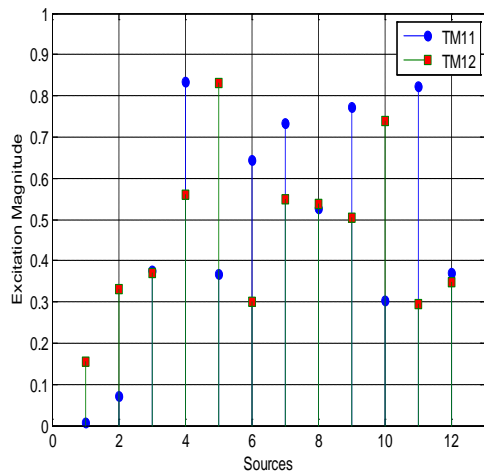


Fig.19 Excitation amplitudes and phases by APSO for the two modes.

Our proposed method can be extended to the planar antenna array which consists of 10×10 annular ring antennas equally spaced by 0.5λ along

the directions O_x and O_y . The synthesis objective was to obtain a pattern with two narrow beams in the desired directions for the two modes TM_{11} and TM_{12} , by acting on the amplitudes and phases of sources while achieving a minimum peak sidelobe level. Satisfactory results were obtained and multibeam patterns were achieved and plotted in the polar coordinate system, as shown in figures 20 and 21.

The excitation amplitudes and phases of the elements are depicted in figures 24 and 25, for both modes TM_{11} and TM_{12} . For the design specifications, the modified particle swarm optimization method is run for 200 iterations, for both modes TM_{11} and TM_{12} .

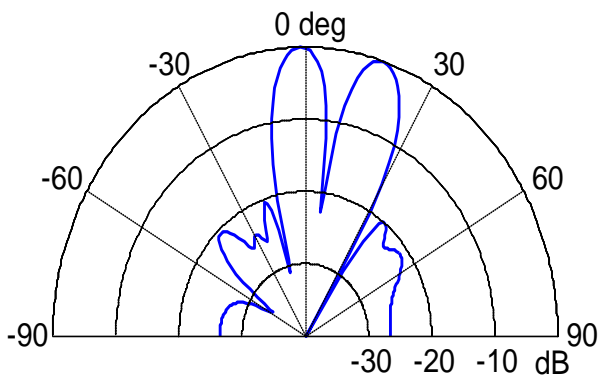


Fig.20 Normalized pattern TM_{11}

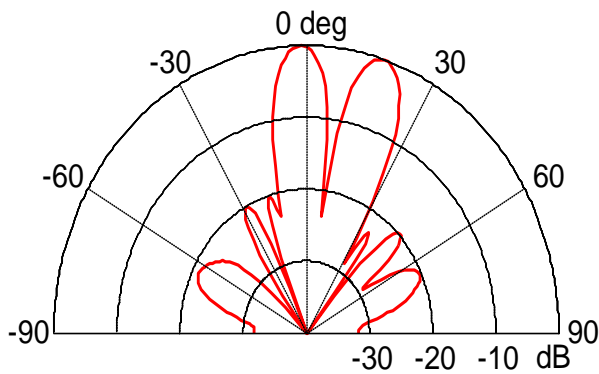


Fig.21 Normalized pattern TM_{12} .

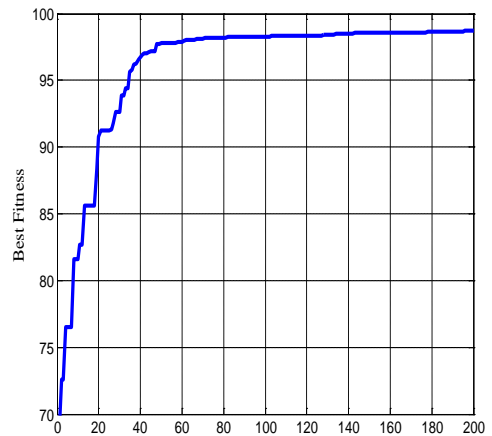


Fig.22 The convergence curve TM_{11} .

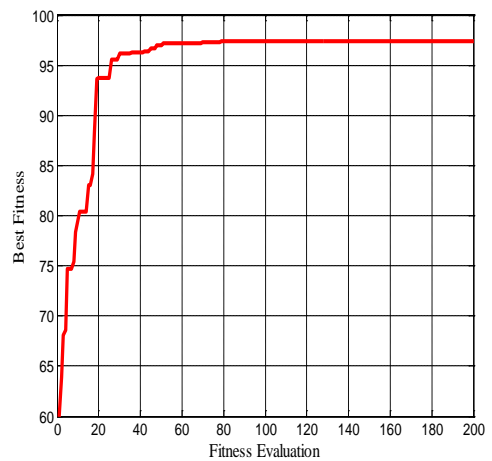
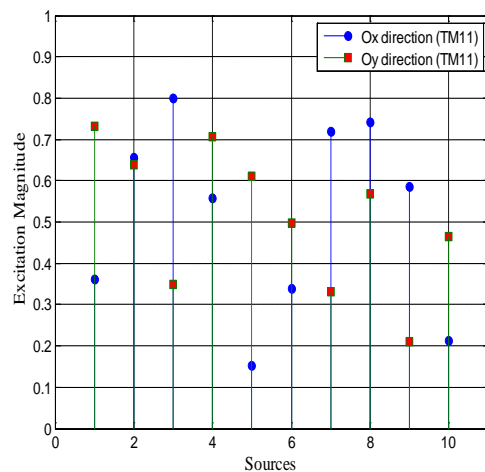


Fig.23 The convergence curve TM_{12} .



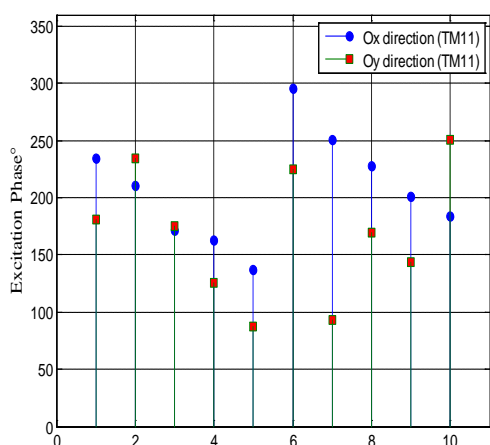


Fig.24 Excitation amplitudes and phases for the TM₁₁ mode according to the two directions

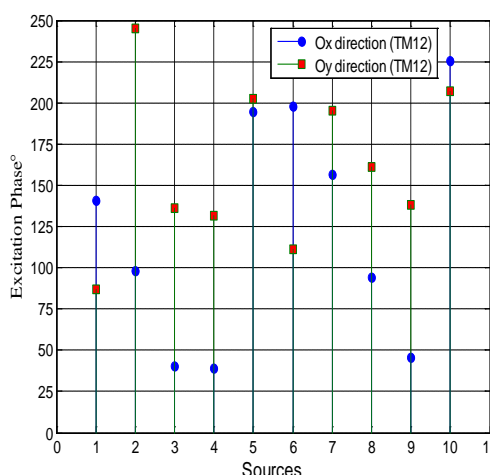
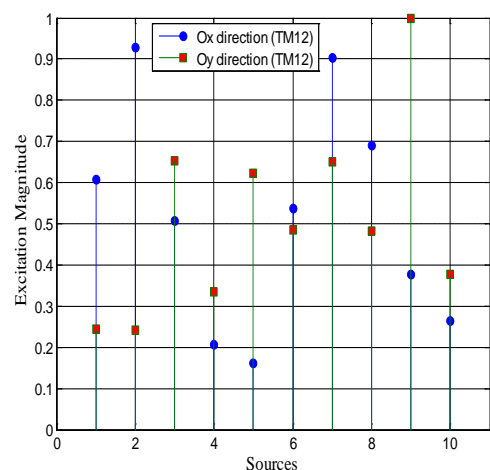


Fig.25 Excitation amplitudes and phases for the TM₁₂ mode according to the two directions

The synthesis examples highlight the main features of our proposed method. These arrays satisfy stringent requirements, especially in terms of

maximum directivity to be guaranteed in the desired angles and the side lobe levels to be kept below an assigned value.

4 Conclusion

This paper presents a rigorous synthesis of multibeam annular ring antenna arrays using the adaptive particle swarm optimization algorithm for two modes TM₁₁ and TM₁₂. An acceptable side lobe level (SLL) was obtained while high directivities and narrow beams were achieved. Results show a very good agreement between the desired and the synthesized specifications, for the two modes. Important results showed the effectiveness of the proposed adaptive swarm optimization algorithm in finding the optimized complex weight vectors.

References:

- [1] R. J. Mailloux, *Phased Array Antenna Handbook*, Artech House, Boston, 2005.
- [2] J.S Dahele and K.F Lee, Theory and Experiment on Microstrip Antennas with Airgaps, *IEE Proceedings*, Vol. 132, No. 7, 1985, pp. 455-460.
- [3] G. A. Deschamps, *Microstrip Microwave Antennas*, Proc. 3rd USAF Symposium on Antennas, 1953.
- [4] H. Chaker, S M. Meriah and F T. Bendimerad, One and Two Dimensions Unequally Array Pattern Synthesis with the use of a Modified Particle Swarm Optimization Algorithm, *WSEAS Transactions on Communications*, Vol. 11, Issue 6, 2012, pp.207-217.
- [5] H. Chaker, SM. Meriah and F T. Bendimerad, Optimization of Micro Strip Array Antennas Using Hybrid Particle Swarm Optimizer with Breeding and Subpopulation for Maximum Side Lobe Reduction, *RADIOENGINEERING*, VOL.17, No.4, 2008, pp. 39-44.
- [6] H. Chaker, SM. Meriah and F T. Bendimerad, Synthesis of Multibeam Antennas Arrays with a Modified Particle Swarm Optimization Algorithm, *The International Arab Journal of Information Technology*, Vol.7, No.3, 2010, pp.250-255.
- [7] H. Chaker, Null Steering and Multi-beams Design by Complex Weight of antennas Array with the use of APSO-GA, *WSEAS Transactions on Communications*, Vol. 13, Issue 1, 2014, pp.99-108.
- [8] M. Abri, N. Boukli-hacene and F.T. Bendimerad, Ring Printed Antennas Arrays Radiation. Application to Multibeam,

Mediterranean Microwave Symposium-mms'2004, Marseille, France, 06- 2004.

- [9] R. J. Mailloux, *Electronically Scanned Array*, Morgan and Claypool Pub, 2007.
- [10] X. Xiao-Feng, Z. Wen-Jun and Y. Zhi-Lian, Adaptive Particle Swarm Optimization on Individual Level, *International Conference on Signal Processing, Beijing, China, 2002*, pp. 1215-1218.
- [11] J. Kennedy, The Particle Swarm: Social Adaptation of knowledge, *IEEE Int. Conf. on Evolutionary Computation*, 1997, pp.303-308.
- [12] R. Eberhart and Y. Shi, Particle Swarm Optimization: Developments, Applications and Resources. *IEEE Int. Conf. on Evolutionary Computation*, 2001, pp.81-86.
- [13] G. Nicolis, and Prigogine, Self-organization in no Equilibrium Systems: from Dissipative Systems to order Through Fluctuations, *John Wiley*, NY, 1977.